Supplement of Atmos. Chem. Phys., 22, 15207–15221, 2022
https://doi.org/10.5194/acp-22-15207-2022-supplement

Atmospheric
Chemistry
and Physics
Open Access

Supplement of

Aerosol–cloud interaction in the atmospheric chemistry model GRAPES_Meso5.1/CUACE and its impacts on mesoscale numerical weather prediction under haze pollution conditions in Jing–Jin–Ji in China

Wenjie Zhang et al.

Correspondence to: Hong Wang (wangh@cma.gov.cn)

Supplement

Sect. S1 Implementation of ACI in the model

S1.1 The supersaturation degree

In the Thompson cloud microphysics scheme, the supersaturation degree (S) is obtained by the following function (1):

$$\mathrm{S} = \left(\frac{q}{q_s} - 1\right) \times 100\% \qquad (1),$$

where q and q_s represent the water vapor mixing ratio and the saturation water vapor mixing ratio. The q_s is given by the function (2) and (3):

$$q_s = \frac{0.622 \times e_{sw}}{p - e_{sw}} \qquad (2),$$

$$e_{sw} = 6.112 \times \exp\left\{17.67 \times \left(\frac{T-273.16}{T-29.65}\right)\right\} \qquad (3),$$

where e_{sw} is the saturated vapour pressure over water (hPa), p is the air pressure (hPa), and T is the air temperature (K).

S1.2 The cloud droplets activation

In the new Thompson cloud microphysics scheme, when the supersaturation degree is greater than 0, the water-friendly aerosol can be activated as cloud droplets by equation (4):

$$\mathrm{Activ\_Nc} = \mathrm{NWFA} \times \mathrm{AF} \qquad (4),$$

where Activ_Nc represents activated cloud droplets, NWFA represents the number concentration of water-friendly aerosol, and AF represents activated fraction. The activation fraction is determined by the simulated ambient temperature (K), vertical velocity (m/s), number concentration of water-friendly aerosol (cm^{-3}), and pre-determined values of the hygroscopicity parameter (0.4) and aerosol mean radius (0.04 μm) by using a lookup table. This lookup table is created by the explicit treatment of Köhler activation theory using different number concentration of water-friendly aerosol (10.0, 31.6, 100.0, 316.0, 1000.0, 3160.0, 10000.0 cm^{-3}), vertical velocity (0.01, 0.0316, 0.1, 0.316, 1.0, 3.16, 10.0, 31.6, 100.0 m/s), temperature (243.15, 253.15, 263.15, 273.15, 283.15, 293.15, 303.15 K), aerosol mean radius (0.01, 0.02, 0.04, 0.08, 0.16 μm), and hygroscopicity parameter (0.2, 0.4, 0.6, 0.8) according to previous studies (Feingold and Heymsfield, 1992; Thompson and Eidhammer, 2014).

S1.3 The ice nucleation

The real-time cloud ice nucleation is not activated in the current cloud microphysics scheme because of the lack of dust forecast. However, the nucleation of cloud ice due to deposition and condensation freezing is still predicted in the model by the following equation (5) (Cooper, 1986; Thompson et al., 2004) when the supersaturation with respect to ice exceeds 5% or the supersaturation with respect to water exceeds 0 and ambient temperature < -5 ℃:

$$\mathrm{Ni\_d} = 0.005 \times \exp\{0.304 \times (273.15 - T)\} \qquad (5),$$

where Ni_d is the number of ice crystals (/L) and T is the simulated ambient temperature (K). In the future, when the dust module is coupled into the GRAPES_Meso5.1/CUACE model, we will continue to add real-time ice nucleation.

S1.4 The wet scavenging of aerosol and evaporation of cloud droplets

The wet scavenging of aerosol can be divided into the in-cloud and below-cloud scavenging. We calculate the in-cloud scavenging process of aerosol by the collision-coalescence process between aerosol and raindrops (Giorgi and Chameides, 1986). The evaporation of raindrops will lead to returned aerosol. In the below-cloud scavenging process, the removal of aerosol is calculated by using the rain/snow scavenging rate according to previous studies (Slinn, 1977; Gong et al, 1997). All of these wet scavenging processes are activated in the CUACE aerosol module and can give real-time feedback to the aerosol field. The activation of aerosol as cloud droplets does not update the aerosol field in the current model version. In the future, we will complete this process in the GRAPES_Meso5.1/CUACE model and study the impact of ACI on aerosol in detail.

Table S1: The specified values of the tracer number, aerosol types, mean radius (r), and density (ρ).

Tracer number	Aerosol types	Mean radius (μm)	Density (g cm^{-3})
1	OC1	0.0075	1.30
2	OC2	0.015	1.30
3	OC3	0.03	1.30
4	OC4	0.06	1.30
5	OC5	0.12	1.30
6	OC6	0.24	1.30
7	OC7	0.48	1.30
8	OC8	0.96	1.30
9	OC9	1.92	1.30
10	OC10	3.84	1.30
11	OC11	7.68	1.30
12	OC12	15.36	1.30
13	SS1	0.0075	2.17
14	SS2	0.015	2.17
15	SS3	0.03	2.17
16	SS4	0.06	2.17
17	SS5	0.12	2.17
18	SS6	0.24	2.17
19	SS7	0.48	2.17
20	SS8	0.96	2.17
21	SS9	1.92	2.17
22	SS10	3.84	2.17
23	SS11	7.68	2.17
24	SS12	15.36	2.17
25	SF1	0.0075	1.79
26	SF2	0.015	1.79
27	SF3	0.03	1.79
28	SF4	0.06	1.79
29	SF5	0.12	1.79
30	SF6	0.24	1.79
31	SF7	0.48	1.79
32	SF8	0.96	1.79
33	SF9	1.92	1.79
34	SF10	3.84	1.79
35	SF11	7.68	1.79
36	SF12	15.36	1.79
37	NT1	0.0075	1.77
38	NT2	0.015	1.77
39	NT3	0.03	1.77
40	NT4	0.06	1.77

41	NT5	0.12	1.77
42	NT6	0.24	1.77
43	NT7	0.48	1.77
44	NT8	0.96	1.77
45	NT9	1.92	1.77
46	NT10	3.84	1.77
47	NT11	7.68	1.77
48	NT12	15.36	1.77
49	AM	0.06	1.69

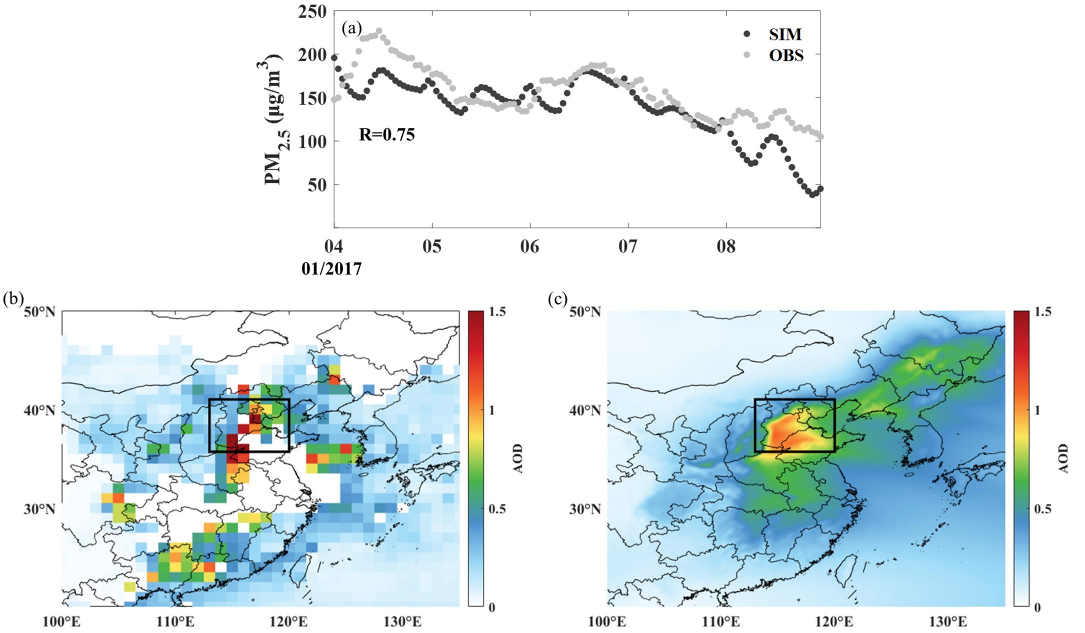

Figure S1: (a) The temporal variation of regional mean $PM_{2.5}$ mass concentration in Jing-Jin-Ji. The (b) observed and (c) simulated by the E1 experiment spatial distribution of mean AOD from 4 to 8 January 2017. The black rectangle represents the location of Jing-Jin-Ji.

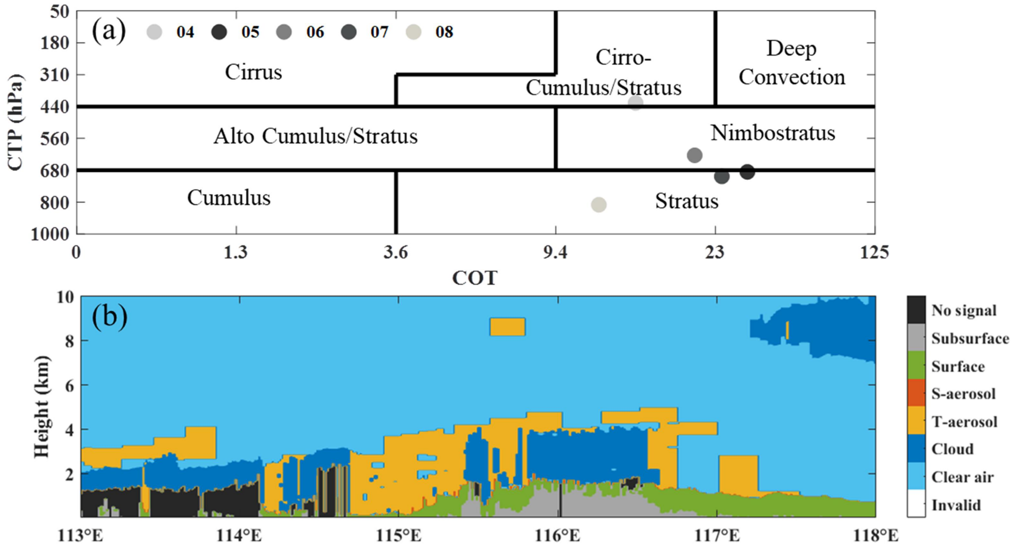

Figure S2: (a) Cloud types over Jing-Jin-Ji from 4 to 8 January 2017 based on ISCCP cloud classification algorithm. (b) The vertical distribution of aerosol and cloud layers described by VFM in Jing-Jin-Ji at 18:12 on 7 January 2017.

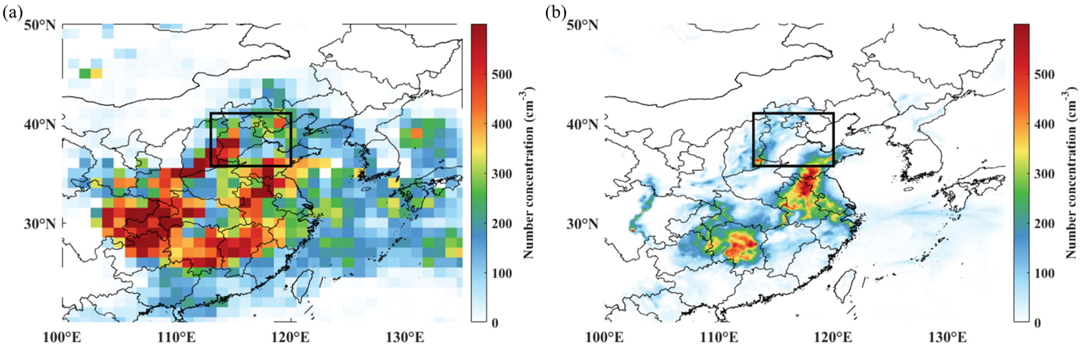

Figure S3: The spatial distribution of mean number concentration of cloud droplets on 7 January 2017. (a) The VIIRS. (b) The mean simulations between 950 and 850 hPa from E2 experiment.

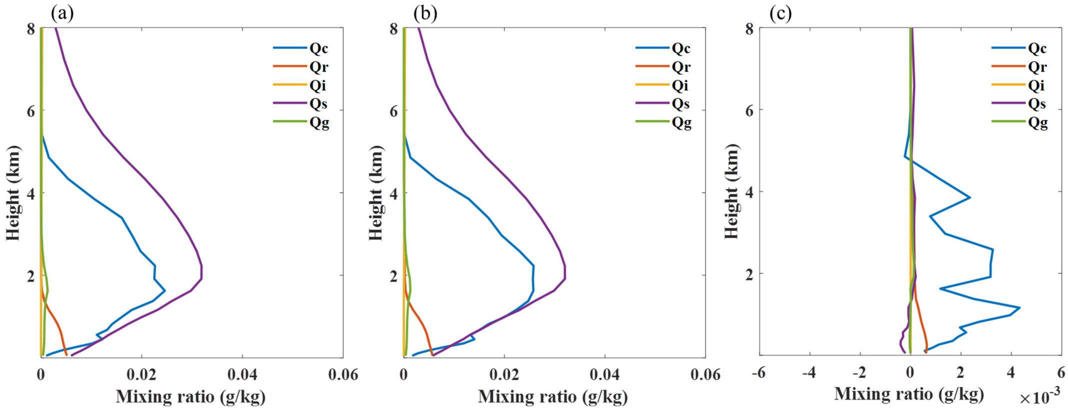

Figure S4: The vertical profile of regional mean hydrometeors mixing ratio (Qc, Qr, Qi, Qs, and Qg) in Jing-Jin-Ji on 7 January 2017. (a) The E1 experiment. (b) The E2 experiment. (c) The difference between the E2 and E1 experiment.

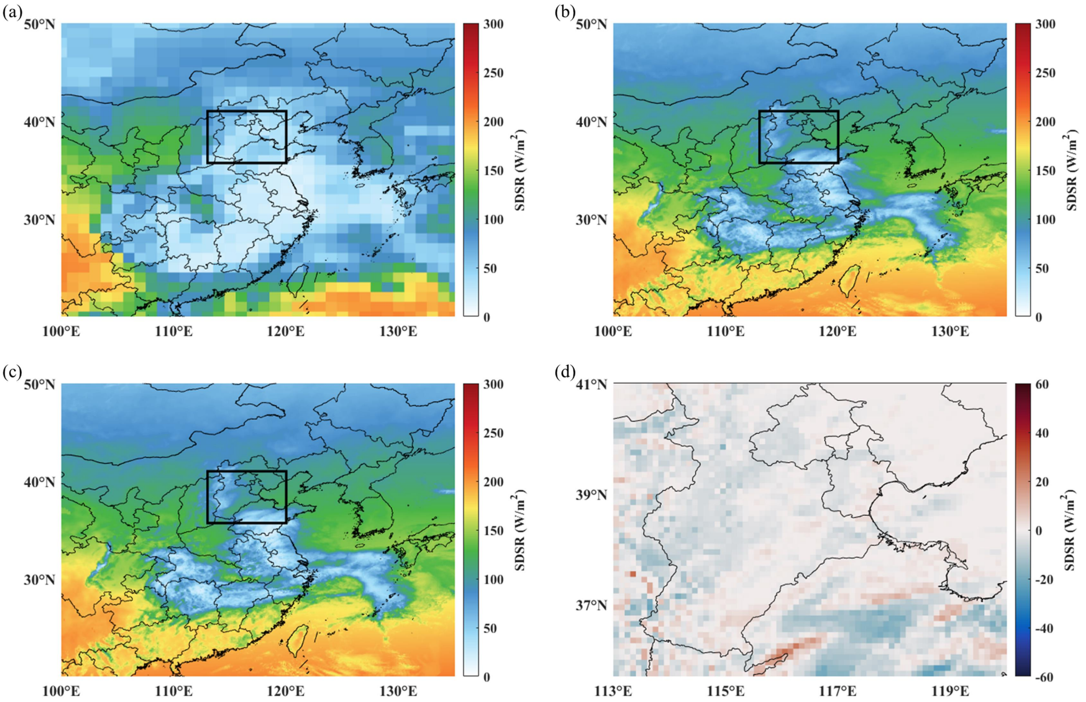

Figure S5: The spatial distribution of mean SDSR on 7 January 2017. (a) The VIIRS. (b) The E1 experiment. (c) The E2 experiment. (d) The difference between the E2 and E1 experiment in Jing-Jin-Ji.

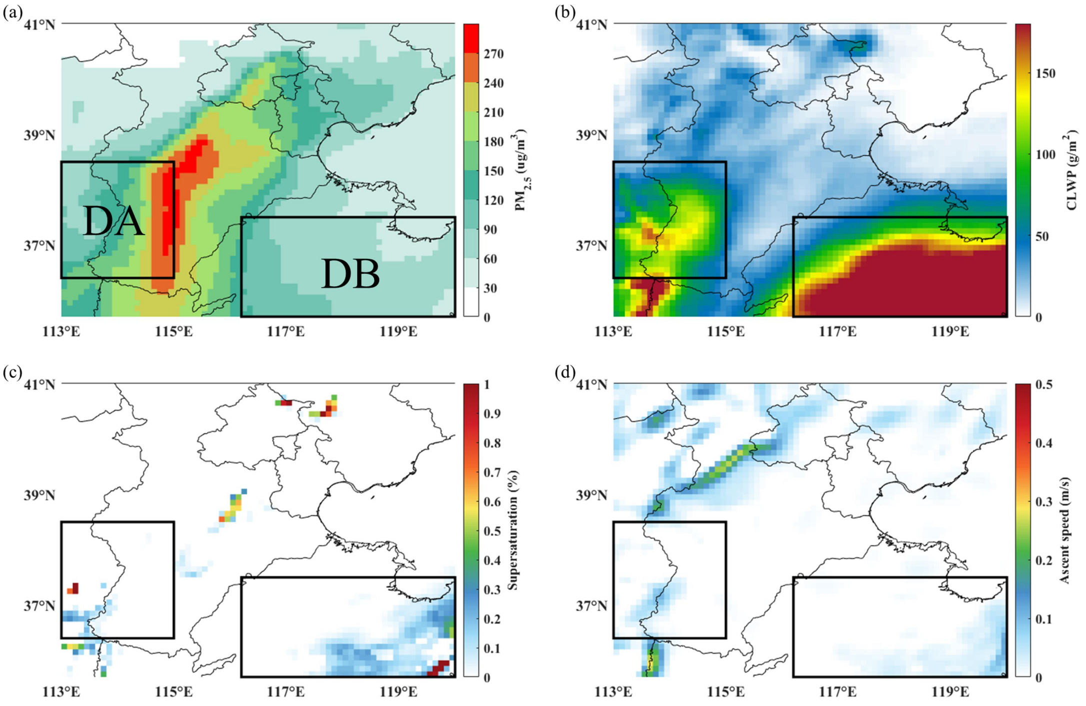

Figure S6: The spatial distribution of $PM_{2.5}$ mass concentration, CLWP, supersaturation (900 hPa), and ascent speed (900 hPa). (a) and (b) mean simulations on 7 January 2017. (c) and (d) simulations at 18:00 on 7 January 2017. The black rectangles are the locations of DA and DB.

Sect. S2 The analysis of the source/sink of rainwater in the cloud microphysical scheme

In the Thompson cloud microphysics scheme, the source/sink of rainwater is calculated by the following equation (6):

Rain tendency= prr_wau + prr_rcw + prr_sml + prr_gml + prr_rcs + prr_rcg - prg_rfz - pri_rfz - prr_rci (6),

where prr_wau is the autoconversion of cloud water to form rain, prr_rcw is the rain collecting cloud water, prr_sml is the melting of snow to form rain, prr_gml the is melting of graupel to form rain, prr_rcs is the rain collecting snow, prr_rcg is the rain collecting graupel, prg_rfz is the freezing of rainwater into graupel, pri_rfz is the freezing of rainwater into ice, and prr_rci is the rain collecting ice. All of these processes lead to changes in rainwater.

Figure S7 shows the difference in mean hydrometeors mixing ratio and rain tendency processes between the E2 (ACI) and E1 (NO-ACI) experiment. In the DA, the largest contribution to the decrease in precipitation is the prr_sml, followed by the prr_rcs and other processes (Figure S7 (c)). In the DB, the largest contribution to the increase in precipitation is also the prr_sml, followed by the prr_rcw and other processes (Figure S7 (d)). In summary, the increase or decrease in simulated precipitation due to the ACI is mainly caused by the melting of snow to form rain (i.e., prr_sml), followed by other source/sink processes of rainwater.

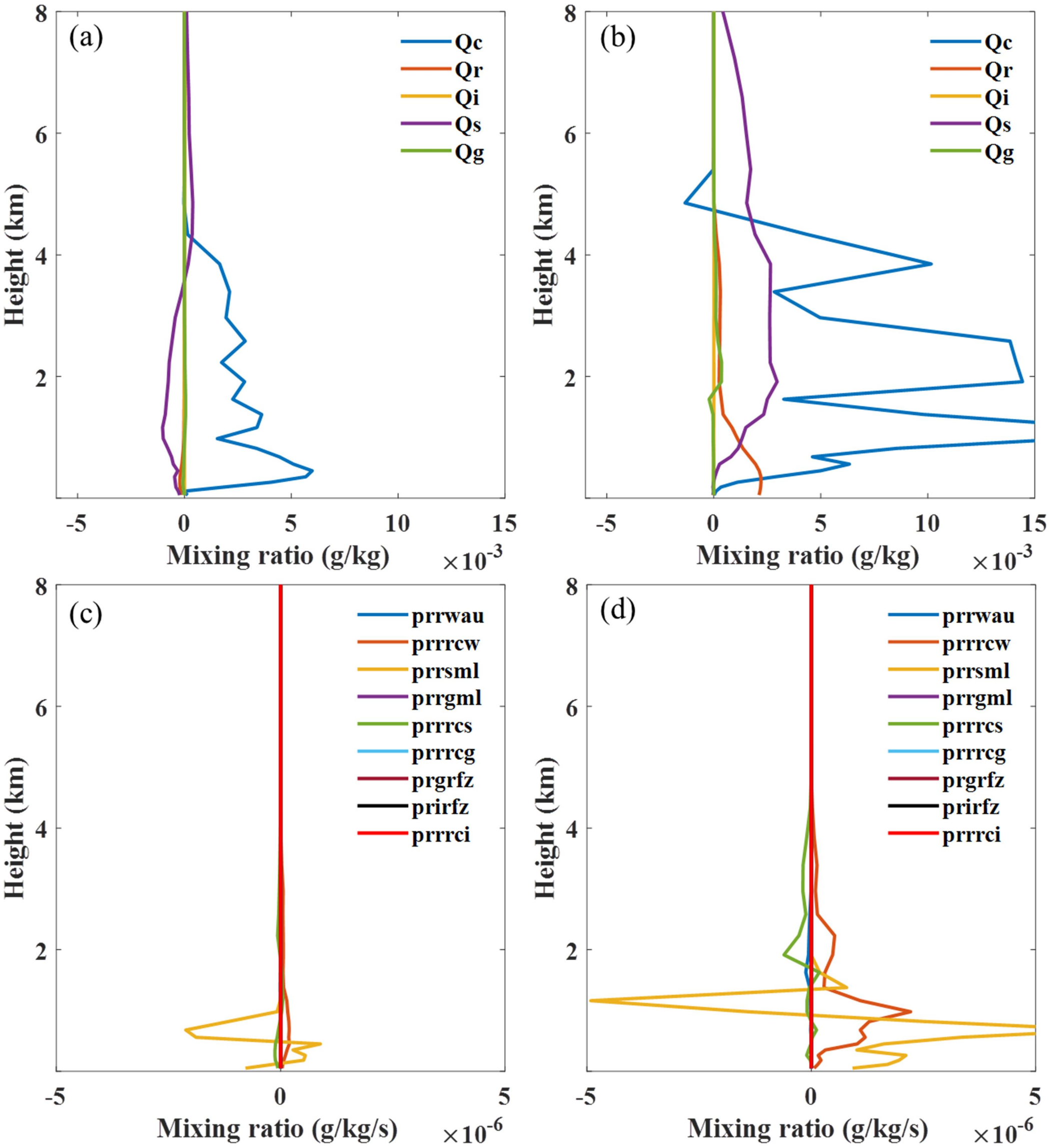

Figure S7: The difference of mean hydrometeors mixing ratio (top) and rain tendency processes (bottom)

between the E2 and E1 experiment on 7 January 2017 in the (a and c) DA and (b and d) DB.

References

Cooper, W. A.: Ice initiation in natural clouds, Precipitation Enhancement—A Scientific Challenge, Meteor. Monogr., No. 43, Amer. Meteor. Soc., 29–32, 1986.

Feingold, G., and Heymsfield, A. J.: Parameterizations of condensational growth of droplets for use in general circulation models. J. Atmos. Sci., 49, 2325–2342, https://doi.org/10.1175/1520-0469(1992)049,2325:POCGOD.2.0.CO;2, 1992.

Giorgi, F., and Chameides, W. L.: Rainout lifetimes of highly soluble aerosols and gases as inferred from simulations with a general circulation model, J. Geophys. Res., 91, 14367– 14376, https://doi.org/10.1029/JD091iD13p14367, 1986.

Gong, S. L., Barrie, L. A., and Blanchet, J.-P.: Modeling sea-salt aerosols in the atmosphere: 1. Model development, J. Geophys. Res., 102, 3805–3818, https://doi.org/10.1029/96JD02953, 1997.

Slinn, W.G.N: Some approximations for the wet and dry removal of particles and gases from the atmosphere, Water Air Soil Pollut, 7, 513–543, https://doi.org/10.1007/BF00285550, 1977.

Thompson, G. and Eidhammer, T.: A Study of Aerosol Impacts on Clouds and Precipitation Development in a Large Winter Cyclone, Journal of the Atmospheric Sciences, 71, 3636-3658, https://doi.org/10.1175/JAS-D-13-0305.1, 2014.

Thompson, G., Rasmussen, R. M., and Manning, K.: Explicit forecasts of winter precipitation using an improved bulk microphysics scheme. Part I: Description and sensitivity analysis, Mon. Wea. Rev., 132, 519-542, 2004.